



Article

Probing Our Universe's Past Using Earth's Geological and Climatological History and Shadows of Galactic Black Holes

V. K. Oikonomou ^{1,2,*} , Pyotr Tsyba ² and Olga Razina ² 

¹ Department of Physics, Aristotle University of Thessaloniki, 54124 Thessaloniki, Greece

² Department General and Theoretical Physics, L. N. Gumilyov Eurasian National University, Nur-Sultan 010000, Kazakhstan

* Correspondence: v.k.oikonomou1979@gmail.com or voikonomou@auth.gr or voiko@physics.auth.gr

Abstract: In this short review, we discuss how Earth's climatological and geological history and also how the shadows of galactic black holes might reveal our Universe's past evolution. Specifically we point out that a pressure singularity that occurred in our Universe's past might have left its imprint on Earth's geological and climatological history and on the shadows of cosmological black holes. Our approach is based on the fact that the H_0 tension problem may be resolved if some sort of abrupt physics change occurred in our Universe 70–150 Myrs ago, an abrupt change that deeply affected the Cepheid parameters. We review how such an abrupt physics change might have been caused in our Universe by a smooth passage of it through a pressure finite-time singularity. Such finite-time singularities might occur in modified gravity and specifically in $F(R)$ gravity, so we show how modified gravity might drive this type of evolution, without resorting to peculiar cosmic fluids or scalar fields. The presence of such a pressure singularity can distort the elliptic trajectories of bound objects in the Universe, causing possible geological and climatological changes on Earth, if its elliptic trajectory around the Sun might have changed. Also, such a pressure singularity affects directly the circular photon orbits around supermassive galactic black holes existing at cosmological redshift distances, thus the shadows of some cosmological black holes at redshifts $z \leq 0.01$, might look different in shape, compared with the SgrA* and M87* supermassive black holes. This feature however can be checked experimentally in the very far future.

Keywords: hubble tension; sudden singularity; pressure singularity; cosmological singularities; black hole shadow; modified gravity



Citation: Oikonomou, V.K.; Tsyba, P.; Razina, O. Probing Our Universe's Past Using Earth's Geological and Climatological History and Shadows of Galactic Black Holes. *Universe* **2022**, *8*, 484. <https://doi.org/10.3390/universe8090484>

Academic Editors: Leandros Perivolaropoulos, Eleonora Di Valentino and Jackson Levi Said

Received: 30 August 2022

Accepted: 9 September 2022

Published: 14 September 2022

Publisher's Note: MDPI stays neutral with regard to jurisdictional claims in published maps and institutional affiliations.



Copyright: © 2022 by the authors. Licensee MDPI, Basel, Switzerland. This article is an open access article distributed under the terms and conditions of the Creative Commons Attribution (CC BY) license (<https://creativecommons.org/licenses/by/4.0/>).

1. Introduction

The H_0 -tension is an old problem in physics which still troubles theoretical cosmologists, since no definite solution has proven to solve it. Specifically, the tension on the H_0 value exists between the large redshift sources like the Cosmic Microwave Background (CMB) radiation [1] and the small redshift sources like the Cepheids [2]. Currently, the H_0 tension problem is quite timely and there exists a large stream of research works which try to explain theoretically the tension, see for example [3–38]. It is notable that the H_0 -tension might be a problem of calibration of the Cepheids [3,18], however no solid proof on any aspect is given to date.

Recently it has been noted that an abrupt change in the global physics of the Universe that occurred nearly 70–150 Myrs ago, it might explain in an appealing way the H_0 -tension problem [3,8,10]. Following this line of research, in [11,12] we investigated how such an abrupt global physics change might have been caused in our Universe's past due to the occurrence of a pressure finite-time cosmological singularity, also known as sudden or Type II singularities. These cosmological singularities are rather smooth, causing definable features in the Universe's recent past, which could have had a direct impact on Earth's climatological and geological history and also might have directly affected the shadows of

cosmological black holes corresponding exactly to this redshift 70–150 Myrs ago. Pressure singularities are global events in the Universe, because these singularities occur at a finite time instance $t = t_s$ and occur globally on the 3-dimensional spacelike hypersurface at $t = t_s$. In this paper we shall review these possible scenarios for our Universe's past and we bring together all the material needed for this review. Specifically, we shall show that these pressure singularities naturally occur in modified gravity and specifically $F(R)$ gravity. Also, such finite-time singularities affect the orbits of bound objects in the Universe. Thus, it might be possible that if such a singularity occurred 70–150 Myrs ago, might have affected Earth's elliptic orbit around the Sun, and in effect, the climate on Earth might have changed globally, or even the strong tidal effects might have changed abruptly the geology of Earth. On the other hand, at larger scales, a pressure singularity might have affected the photon orbits around cosmological supermassive black holes, and in effect their shadows. In order to model this, we shall use the McVittie metric [39–53] because it is a consistent description for a black hole in an expanding spacetime. Indeed, the Universe's expansion should affect the cosmological black holes and the only consistent metric that describes such an inhomogeneity in an expanding Universe is the McVittie metric. Some time ago it was debatable whether the McVittie metric truly described a black hole [40], nowadays it is certain that the McVittie metric describes a black hole in an expanding Universe [41,49,50,52,53]. As we show, the photon orbits around supermassive McVittie black holes are directly affected by a pressure singularity, thus this may have definable features on their shadow. The shadows of supermassive black holes are gradually developing to be quite fruitful for new physics discoveries, see for example [54–61] and references therein.

2. Pressure Singularities in our Universe's Past and $F(R)$ Gravity

Pressure singularities are rather smooth cosmological singularities which are geodetically complete, and moreover the strong energy conditions are respected during the passage of the Universe through them. The classification of cosmological finite-time singularities was made in [62], so by assuming that the cosmic singularity occurs at $t = t_s$, finite-time singularities are classified as follows:

- Type I ("The Big Rip") : This is a severe singularity of crushing type at $t = t_s$, at which all the physical observable quantities blow up, and specifically the pressure, the energy density and the scale factor [63–65].
- Type II ("The Sudden Singularity") : This is the pressure singularity which we shall consider in this review, see Refs. [66–70] for details. In this case, the scale factor and the energy density remain finite at $t = t_s$ while the pressure diverges.
- Type III : This is also a crushing type singularity, in which case the pressure and the energy density diverge while the scale factor remains finite.
- Type IV : This is a soft singularity in which case all the observable quantities remain finite on the three dimensional spacelike hypersurface defined by the condition $t = t_s$ [62,71–75], and only the higher derivatives of the Hubble rate diverge, that is $\frac{d^n H}{dt^n} \rightarrow \infty$, for $n \geq 2$.

In order to further understand what a pressure singularity is and how this singularity can be realized by cosmological systems, let us assume that the scale factor of the Universe has the following form,

$$a(t) \simeq g(t)(t - t_s)^\alpha + f(t), \quad (1)$$

with $g(t)$ and $f(t)$ are smooth functions of the cosmic time, and the same applies for all their higher derivatives. For consistency, let us assume that $\alpha = \frac{2m}{2n+1}$, in order to avoid having complex values for the scale factor, so according to the classification of finite-time singularities listed above, depending on the values of α , we may have these singularities for the scale factor (1):

- For $\alpha < 0$ a Type I singularity is developed.
- For $0 < \alpha < 1$ a Type III singularity is developed.

- For $1 < \alpha < 2$ a Type II singularity is developed.
- For $2 < \alpha$ a Type IV singularity is developed.

The case we are interested in, that is the pressure singularity, is developed for $1 < \alpha < 2$, since the first derivative of the Hubble rate diverges $\dot{H} \sim \frac{(\alpha-1)\alpha(t-t_s)^{\alpha-2}}{f(t)}$ and the same applies for the second derivative of the scale factor $\ddot{a} \sim (\alpha-1)\alpha g(t)(t-t_s)^{\alpha-2}$. As we already mentioned, for pressure singularities, only the pressure diverges, and these singularities are geodetically complete, since the following quantity is finite [69],

$$\int_0^\tau dt R_{0j0}^i(t). \quad (2)$$

More importantly, we have $\rho_{\text{eff}} + 3p_{\text{eff}} > 0$ and $\rho_{\text{eff}} > 0$, thus the strong energy conditions are not violated when a pressure singularity occurs. In the context of standard general relativity, the above conditions can be realized by a scalar field and several cosmic fluids, but the systems must be severely constrained. In the context of $F(R)$ gravity however, the realization of the (1) and simultaneously satisfying the strong energy conditions is much more easy due to the fact that in the context of $F(R)$ gravity, a geometric fluid does the job in an elegant and simple way. To have a direct grasp on this, let us consider the $F(R)$ gravity action in the presence of perfect matter fluids (cold dark matter and radiation),

$$\mathcal{S} = \frac{1}{2\kappa^2} \int d^4x \sqrt{-g} F(R) + S_m(g_{\mu\nu}, \Psi_m), \quad (3)$$

with $\kappa^2 = 8\pi G$ and also S_m stands for the action of the perfect matter fluids. The field equations can be obtained by varying the action with respect to the metric tensor in the metric formalism, and these are,

$$R_{\mu\nu} - \frac{1}{2} R g_{\mu\nu} = \frac{\kappa^2}{F_R(R)} \left(T_{\mu\nu} + \frac{1}{\kappa^2} \left(\frac{F(R) - R F_R(R)}{2} g_{\mu\nu} + \nabla_\mu \nabla_\nu F_R(R) - g_{\mu\nu} \square F_R(R) \right) \right). \quad (4)$$

with $F_R(R) = \partial F(R)/\partial R$ and also $T_{\mu\nu}$ denotes the energy momentum tensor of the perfect fluids present. The field equations can be cast in the Einstein-Hilbert form in the following way,

$$R_{\mu\nu} - \frac{1}{2} R g_{\mu\nu} = T_{\mu\nu}^m + T_{\mu\nu}^{curv}, \quad (5)$$

with $T_{\mu\nu}^m$ being equal to,

$$T_{\mu\nu}^m = \frac{1}{\kappa} \frac{T_{\mu\nu}}{F_R(R)}, \quad (6)$$

which originates from the perfect fluids, while the energy momentum tensor $T_{\mu\nu}^{curv}$ originates purely from $F(R)$ gravity and it is equal to,

$$T_{\mu\nu}^{curv} = \frac{1}{\kappa} \left(\frac{F(R) - R F_R(R)}{2} g_{\mu\nu} + F_R(R) i^{\mu\nu} (g_{\alpha\mu} g_{\beta\nu} - g_{\alpha\beta} g_{\mu\nu}) \right). \quad (7)$$

What we effectively have at hand is an energy momentum tensor acting as a source of gravity, which has a completely geometric origin coming from $F(R)$ gravity terms.

For the consideration of the distortion of the planetary orbits, we shall assume that the expanding Universe is described by a flat Friedmann-Robertson-Walker (FRW) metric, with the following line element,

$$ds^2 = -dt^2 + a(t)^2 \sum_{i=1,2,3} (dx^i)^2, \quad (8)$$

with $a(t)$ being the scale factor, and with the corresponding Ricci scalar for the FRW metric being

$$R = 6(\dot{H} + 2H^2), \quad (9)$$

where as usual $H = \frac{\dot{a}}{a}$, stands for the Hubble rate. In the same context, the field equations of $F(R)$ gravity for a FRW metric, take the form,

$$\begin{aligned} 3H^2 F_R &= \frac{RF_R - F}{2} - 3H\dot{F}_R + \kappa^2(\rho_r + \rho_m), \\ -2\dot{H}F &= \ddot{F}_R - H\dot{F}_R + \frac{4\kappa^2}{3}\rho_r, \end{aligned} \quad (10)$$

with p_r , ρ_m and ρ_r being the pressure and the total energy densities of the radiation and cold dark matter perfect fluids. We further write the field equations in the Einstein-Hilbert form as follows,

$$\begin{aligned} 3H^2 &= \kappa^2 \rho_{tot}, \\ -2\dot{H} &= \kappa^2(\rho_{tot} + P_{tot}), \end{aligned} \quad (11)$$

with $\rho_{tot} = \rho_m + \rho_G + \rho_r$ being the total energy density, ρ_m is cold dark matter energy density, and ρ_r denotes the radiation perfect fluid energy density. Furthermore, ρ_G denotes the total energy density of the $F(R)$ gravity geometrical fluid which is defined as,

$$\kappa^2 \rho_G = \frac{F_R R - F}{2} + 3H^2(1 - F_R) - 3H\dot{F}_R, \quad (12)$$

and its pressure is,

$$\kappa^2 P_G = \ddot{F}_R - H\dot{F}_R + 2\dot{H}(F_R - 1) - \kappa^2 \rho_G. \quad (13)$$

Effectively, the strong energy conditions are much more easily satisfied in the context of $F(R)$ gravity, by the geometrically generated perfect fluid with energy momentum tensor $T_{\mu\nu}^{curv}$. It is useful to see explicitly what a pressure singularity would imply for a flat FRW Universe. Firstly, before and after the singularity, the Universe can superaccelerate or superdecelerate for a slight amount of time near the singularity, due to the fact that the second derivative of the scale factor diverges at the time instance that the singularity occurs. This feature complies with the abrupt changes in physics of Ref. [76]. Furthermore, another important implication of the pressure singularity would be on the total effective gravitational constant of $F(R)$ gravity. Considering only subhorizon modes, that is modes which satisfy,

$$\frac{k^2}{a^2} \gg H^2, \quad (14)$$

the perturbations of matter density defined by the parameter $\delta = \frac{\delta \varepsilon_m}{\varepsilon_m}$, evolve according to the following differential equation,

$$\ddot{\delta} + 2H\dot{\delta} - 4\pi G_{eff}(a, k)\varepsilon_m \delta = 0, \quad (15)$$

with $G_{eff}(a, k)$ being the total effective gravitational constant of $F(R)$ gravity theory, which has the following form [77],

$$G_{eff}(a, k) = \frac{G}{F_R(R)} \left[1 + \frac{\frac{k^2}{a^2} \frac{F_{RR}(R)}{F_R(R)}}{1 + 3 \frac{k^2}{a^2} \frac{F_{RR}(R)}{F_R(R)}} \right], \quad (16)$$

with G denoting as usual Newton's gravitational constant. Obviously the terms containing the Ricci scalar and functions of it, will directly be affected by a pressure singularity because in a flat FRW spacetime, the Ricci scalar takes the form $R = 12H^2 + 6\dot{H}$, and \dot{H} diverges at a pressure singularity. Hence, this feature also complies with the argument of Ref. [76] of a sudden physics change before 70–150 Myrs which might have changed the Cepheid variables. Also, the change directly on the effective gravitational constant at small redshift as an explanation for the H_0 -tension was also mentioned in Ref. [38].

3. Effects of a Pressure Singularity on Solar System Orbits and the Shadows of Galactic Black Holes

Let us now discuss in a direct and quantitative way the implications of a pressure singularity in the orbits of bound objects and on the shadows of galactic black holes. We start off with the former case, and in such a scenario, the pressure singularity causes tidal forces in gravitationally bound objects in the Universe, resulting in the disturbance of their orbits. This scenario was considered sometime ago in Ref. [76], and now we shall discuss the implications of this scenario on the elliptic curve of Earth around the Sun in our solar system and we shall also discuss the effects of a disruption of Moon's orbit around Earth.

If this scenario indeed occurred 70–150 Myrs ago, then in principle it would have dramatic effects on the climate and the geology of Earth. Indeed, if Earth's orbit around the Sun was disrupted before 70–150 Myrs, extreme temperature changes would occur on the surface of Earth, even an ice age would be justified, and we know that such an era actually occurred. Accordingly, if the orbit of Moon was disrupted, the tidal effects on the surface of Earth would be quite severe, and tides would be so strong that perhaps entire seas would disappear from their original places. In fact, the whole morphology of the surface of the earth would abruptly change, and it is intriguing that the morphological changes on Tethys Sea occurred chronologically nearly 70–150 Myrs ago.

Let us see in a quantitative way how the elliptic orbit could be affected by the occurrence of a pressure finite-time singularity. We shall use the framework developed in Ref. [76], without invoking modified gravity for simplicity. We start from a different orbit compared to Ref. [76], and specifically from an elliptic curve, instead of a circle. Following [76,78], for a FRW Universe, the total energy and pressure are $\rho(t) = \frac{3}{8\pi G} \left(\frac{\dot{a}^2}{a^2} \right)$ and $p(t) = \frac{1}{8\pi G} \left(2\frac{\ddot{a}}{a} + \frac{\dot{a}^2}{a^2} \right)$, hence it is apparent that the pressure becomes singular for a pressure singularity, due to the presence of the second time-derivative of the scale factor. Let us model a pressure singularity in a simple way, so assume that the singularity occurs at $t = 0$ and therefore the pressure singularity could occur if the scale factor has the following form,

$$a(t) = 1 + c|t|^\eta. \quad (17)$$

The values of the parameter η for which the singularity occurs are $1 < \eta < 2$. Consider a gravitational source with mass M , the Newtonian limit of the metric describing the spacetime at the vicinity of this compact object M is [76,78],

$$ds^2 = \left(1 - \frac{2GM}{a(t)\rho} \right) \cdot dt^2 - a(t)^2 \cdot \left(d\rho^2 + \rho^2 \cdot (d\theta^2 + \sin^2\theta d\varphi^2) \right), \quad (18)$$

which is a correct description when $\frac{2GM}{a(t)\rho} \ll 1$ and note that this condition holds true even for pressure singular scale factors, since a is not singular on pressure singularities. Introducing $r = a(t) \cdot \rho$, the equations that determine the geodesics of the spacetime metric (18) are [76,78],

$$\left(\ddot{r} - \frac{\ddot{a}}{a}r \right) + \frac{GM}{r^2} - r\dot{\varphi}^2 = 0, \quad r^2\dot{\varphi} = L \quad (19)$$

where L is the total angular momentum per unit mass, and it is an integral of motion. Using equations (19), we obtain the radial equation of motion of a point particle around the gravitational object with mass M [76,78],

$$\ddot{r} = \frac{\ddot{a}}{a}r + \frac{L^2}{r^3} - \frac{GM}{r^2}. \quad (20)$$

It is vital to study dimensionless quantities, so we perform the following rescalings $\bar{r} \equiv \frac{r}{r_0}$, $\bar{\omega}_0 \equiv \omega_0 t_0$ and $\bar{t} \equiv \frac{t}{t_0}$, with r_0 and t_0 being arbitrary length and time scales. Upon defining $\dot{\varphi}(t_0) = \omega_0 \equiv \frac{GM}{r_0^3}$, the geodesics equation takes the following form [76,78],

$$\ddot{\bar{r}} - \frac{\bar{\omega}_0^2}{\bar{r}^3} + \frac{\bar{\omega}_0^2}{\bar{r}^2} - \frac{\ddot{a}}{a} \bar{r} = 0. \quad (21)$$

For a pressure singularity, the geodesics equation takes the following form,

$$\ddot{\bar{r}} = \frac{\bar{\omega}_0^2}{\bar{r}^3} - \frac{\bar{\omega}_0^2}{\bar{r}^2} + \frac{c \eta (\eta - 1) |\bar{t}|^{\eta-2}}{(c |\bar{t}|^\eta + 1)} \bar{r}. \quad (22)$$

We performed a numerical analysis of the resulting geodesics differential equation, giving various values to the parameters η and c , having in mind the disruption and not the destruction of the bound system. Regarding the initial conditions, we chose the initial orbit to be an elliptic curve. Our results are presented in the three plots of Figure 1. In the upper left panel of Figure 1, we present the trajectory of the test mass around the massive object M , before the singularity, during the pressure singularity and after the pressure singularity. The green curve represents the elliptic orbit of the test mass before the singularity, and at the vicinity of the singularity, a disruption of the orbit occurs, and the orbit is described by the blue curve, resulting to a final elliptic orbit which is different from the initial orbit. In the upper right panel we plot the radial coordinate of the orbit before and after the singularity. Apparently, the two elliptic orbits are distinct before and after the singularity. Finally, in the bottom panel of Figure 1 we present the functional dependence of $\varphi(t)$ with respect to the cosmic time. The same analysis can be carried away for $F(R)$ gravity, but we refrain to analyze this case, because the physics would be qualitatively identical to the present case, and just the analysis would be slightly more difficult to perform.

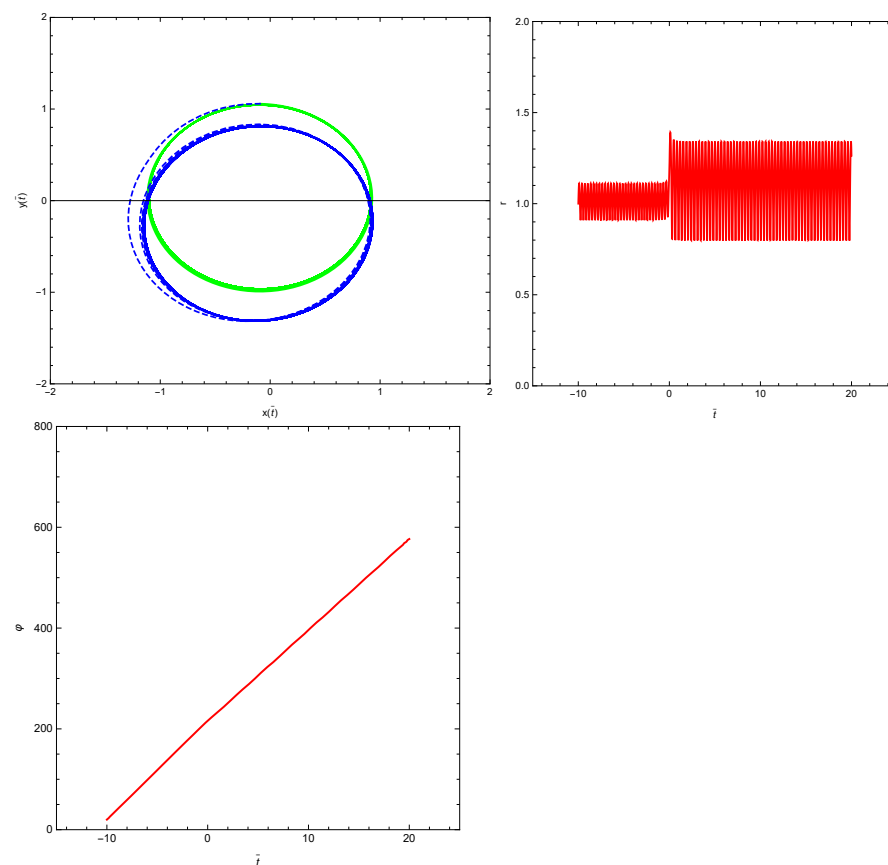


Figure 1. Upper left panel: Point particle trajectories in the Cartesian plane before the pressure singularity (green curves) during the pressure singularity and after the pressure singularity (blue curves). Upper right panel: The functional dependence of the radial coordinate $\bar{r}(t)$ with respect to the rescaled cosmic time. Bottom Panel: the functional dependence of $\varphi(t)$ with respect to the cosmic time.

Now let us discuss how the shadows of black holes may have imprints of an abrupt physics change before 70–150 Myrs. For our study we shall consider the McVittie metric [39–53] which it is widely accepted today that it describes a black hole in an expanding FRW Universe. The line element of the McVittie metric in geometrized units ($G = c = 1$) is,

$$ds^2 = - \left(\frac{1 - \frac{m(t)}{2r}}{1 + \frac{m(t)}{2r}} \right)^2 \cdot dt^2 - \left(1 + \frac{m(t)}{2r} \right)^4 a(t)^2 \cdot \left(dr^2 + r^2 \cdot (d\theta^2 + \sin^2\theta d\varphi^2) \right), \quad (23)$$

with the function $m(t)$ being defined in the following way,

$$m(t) = \frac{m_0}{a(t)}, \quad (24)$$

with m_0 being the mass of the inhomogeneity or simply the central body which is considered embedded in the expanding FRW background. Basically, m_0 is the mass of the black hole, and $a(t)$ is the scale factor of the Universe. Note that when $a = 1$ the McVittie metric becomes identical to the Schwarzschild metric, while when the mass of the central inhomogeneity reduces to zero, the line element of the FRW spacetime is recovered. The best way to investigate changes on the shadow of galactic black holes is via studying the photon orbits around it. So now we will study the photon orbits in the McVittie spacetime, and we shall focus on geodesic paths on the plane determined by the condition $\theta = \frac{\pi}{2}$. Due to the spherical symmetry of spacetime, the angular momentum conservation condition yields,

$$\dot{\phi} = \frac{L}{R^2}, \quad \dot{\theta} = 0, \quad (25)$$

with R being the areal radius coordinate which is defined in the following way,

$$R = a(t)r \left(1 + \frac{m_0}{2ra(t)} \right)^2. \quad (26)$$

The geodesics equation of the circular photon orbits then reads [48],

$$\frac{L^2}{R^2} = (f^2 - g^2) \dot{t}^2, \quad (27)$$

with the functions f and g being defined in the following way [48],

$$f = \sqrt{1 - \frac{2m(t)}{R}}, \quad g = R \left(H + \frac{\dot{m}}{m} (f^{-1} - 1) \right), \quad (28)$$

where H denotes the Hubble rate $H = \frac{\dot{a}}{a}$ as usual. The physical quantity $\chi(R, t) = f^2 - g^2 = g^{\mu\nu} \nabla_\mu r \nabla_\nu R$ stands for the definition of the trapped spacetime regions and untrapped spacetime regions of the total spherically symmetric spacetime. In order for the spacetime to have circular photon orbits with radius R_c for all the cosmic time values, the following condition must hold true [48],

$$\chi(R_c, t) = f^2 - g^2 = 1 - \frac{2m(t)}{R_c} - R_c^2 \left(H(t) + \frac{\dot{m}(t)}{m(t)} \left(\frac{1}{\sqrt{1 - \frac{2m(t)}{R_c}}} - 1 \right) \right)^2 > 0. \quad (29)$$

When $\chi(t, R_c) < 0$, the circular photon orbits do not exist, and we will show, this is exactly what happens near a sudden singularity. Let us take a simple form for the scale factor in order to show this, so assume that,

$$a(t) = c + c|t|^\eta, \quad (30)$$

with c being an arbitrary constant with Geometrized units $[L]^{-1}$ and also we shall make the assumption that $\eta = \frac{2m}{2n+1}$ with the parameters n and m being positive integers, in order to avoid having complex values for the scale factor. The pressure singularity is developed at $t = 0$ when $1 < \eta < 2$, and we chose $t = 0$ to be the singular point for simplicity. Note that this singularity at $t = 0$ might have occurred at some time instance before 70–150 Myrs, and as we will show, depending on the values of the free parameters c and η , the photon orbits with specific radii, and specifically with radii $2m < R_c \leq 3m$, might not exist for a static black hole in an expanding FRW background. We performed a numerical analysis for the behavior of the quantity that determines the existence or not of photon orbits, namely for $\chi(R_c, t)$ in Figure 2, by choosing the parameter η to have the values $\eta = 2$ (right plot) and for $\eta = 5/2$ (left plot), by also choosing $c = 1.5$ in Geometrized units.

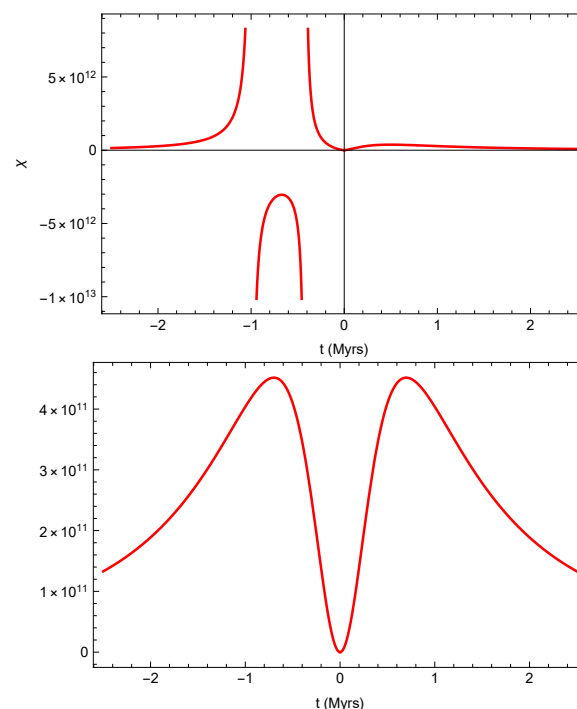


Figure 2. The behavior of the quantity $\chi(R_c, t)$ as a function of the cosmic time, by choosing $R_c = 2.5 m_0$, for the values $\eta = 5/2$ (left plot) and also for $\eta = 2$ (right plot) and by also choosing $c = 1.5$ in Geometrized units. The plot in the left panel depicts the case for which a sudden singularity occurs at the time instance $t = 0$. As it can be seen, the photon orbits do not exist slightly before, during and after the sudden singularity. The numerical analysis was performed for $2m_0 < R_c \leq 3m_0$ and the qualitative picture does not change.

As it can be seen in the left plot of Figure 2, which describes the case that the pressure singularity actually occurs at $t = 0$, the photon orbits exist well before the singularity at $t = 0$, but do not exist slightly before, during and slightly after the singularity. In the right panel of Figure 2, the photon orbits exist before, during and after $t = 0$, because there is no pressure singularity in this case. We performed the same analysis for several values of the photon orbit radii, and specifically for $2m_0 < R_c \leq 3m_0$, but the qualitative picture does not change.

Now the question is what would the absence of photon orbits imply for the shadow of galactic supermassive black holes. The latter are at cosmological distances so they are situated at a non-zero cosmological redshift. The absence of photon orbits would most likely affect the ring of the galactic black hole shadow. Thus if a large sample of galactic black holes is studied, corresponding to redshifts $z \leq 0.01$, if there is a difference between the shadows corresponding to small redshifts compared to the ones corresponding to redshifts $z \sim 0.01$, this could probably indicate that at high redshifts, some global physics

change, like a pressure singularity, might have occurred at the corresponding redshift. However, observing a large sample of galactic black hole shadows at larger redshifts, for the moment is a formidable task, since there exist huge technical difficulties. Currently, the observation of the M87 shadow and of the SgrA* [79–81] is the best that we can get. There exists a large stream of promising works for the shadows of black holes even corresponding to these two galactic black holes, see for example [54–61] and references therein. The M87 black hole exists at $z = 0.004283$ thus due to the limitations on the resolution of VLBI techniques at high redshifts, our proposal cannot be observationally verified at present time, but rather it is a far future proposal.

4. Conclusions

In this short review we discussed a scenario for the late-time Universe in which an abrupt physics change occurred 70–150 Myrs ago, causing a change in the Cepheids variables and thus resolving the H_0 -tension problem. In our approach such an abrupt physics change might have occurred due to a pressure singularity which occurred 70–150 Myrs. The pressure finite-time singularity is a smooth cosmological singularity of timelike form, for which no geodesics incompleteness occurs, and only the pressure diverges on the three dimensional spacelike hypersurface defined by the time instance that the singularity occurs. The strong energy conditions are not violated, and we discussed the implications of such a singularity if this is realized by an $F(R)$ gravity. Indeed, cosmological singularities can easily be realized by $F(R)$ gravity and also the strong energy conditions are also easily satisfied by the geometric fluid generated by the $F(R)$ gravity. One of the notable effects of a pressure singularity realized by $F(R)$ gravity, is the fact that the effective gravitational constant blows up, and this feature is perfectly aligned with the abrupt transition in physics argument of Ref. [38]. Notable and interesting is also the fact that there possibly exists a connection between our approach with the maximum turn around radius in the context of $F(R)$ gravity, see for example [82], see also [83] for relevant cosmographic studies.

Assuming that a pressure singularity occurred in the recent past of our Universe, we discussed in a qualitative way the effects of this type of cosmological singularity on Earth's climate and geological history and on the shadows of cosmological black holes. Starting with the former scenario, if a pressure singularity indeed occurred before 70–150 Myrs, it would globally affect the orbits of compact objects. In such a scenario, both Earth's elliptic curve around the Sun and the Moon's orbit around Earth would be affected. In such a case, the distortion of Earth's orbit around the Sun would cause radical changes on Earth's climate globally, causing in the most extreme scenario instant freezing on the surface of the Earth. Accordingly, the distortion of Moon's orbit around the Earth could cause tidal forces on the surface of the Earth, which could reform the morphology of the surface of the Earth, perhaps even dislocating entire seas.

Regarding the effects of a pressure singularity on the shadow of a galactic black hole at a specific cosmological redshift, we studied the existence of photon orbits around static black holes in an expanding spacetime. As we showed, the photon orbits are affected slightly before, during and slightly after the occurrence of the pressure singularity. Thus if our scenario is indeed true, this could have a measurable effect on cosmological black holes which emitted light before 70–150 Myrs ago, thus at a specific redshift. These supermassive galactic black holes would have different shadows compared with the already mapped M87 and SgrA*. However, our proposal cannot be verified at present time because the resolution of the VLBI techniques forbid analyzing galactic black holes at higher redshifts. In the far future however, such a scenario could be analyzed in more detail for redshifts up to $z \leq 0.01$ and there are further extensions of our simple description we reviewed here. One should take into account the fact that the shadow is a dynamical object, and is thus non-static [49,50,52,53]. The effects of the cosmic expansion on the diameter of the black hole should also be taken into account [47]. Regardless that our proposal seem to belong to a far future to be checked proposal, the current studies are interesting because already up to the present time observations of high redshift galactic black holes already exist [84],

and it is expected that these galactic black holes have large size shadows [49]. Perhaps also the James Webb Space telescope can pin point properties of large redshift supermassive black holes. The techniques used to obtain the shadows of supermassive black holes are continuously developed [85,86] and furthermore theoretical and other aspects are also being refined [54–61,87,88].

Author Contributions: All authors contributed equally. All authors have read and agreed to the published version of the manuscript.

Funding: This research is funded by the Committee of Science of the Ministry of Education and Science of the Republic of Kazakhstan (Grant No. AP14869238).

Institutional Review Board Statement: Not applicable.

Informed Consent Statement: Not applicable.

Data Availability Statement: No new data are used or reported.

Conflicts of Interest: The authors declare no conflict of interest.

References

1. Aghanim N.; et al. [Planck]. Planck 2018 results. VI. Cosmological parameters. *Astron. Astrophys.* **2020**, *641*, A6.
2. Riess, A.G.; Casertano, S.; Yuan, W.; Bowers, J.B.; Macri, L.; Zinn, J.C.; Scolnic, D. Cosmic Distances Calibrated to 1% Precision with Gaia EDR3 Parallaxes and Hubble Space Telescope Photometry of 75 Milky Way Cepheids Confirm Tension with Λ CDM. *Astrophys. J. Lett.* **2021**, *908*, L6. [[CrossRef](#)]
3. Perivolaropoulos, L.; Skara, F. Challenges for Λ CDM: An update. *arXiv* **2021**, arXiv:2105.05208.
4. Perivolaropoulos, L.; Skara, F. A reanalysis of the latest SH0ES data for H_0 : Effects of new degrees of freedom on the Hubble tension. *arXiv* **2022**, arXiv:2208.11169.
5. Reeves, A.; Herold, L.; Vagnozzi, S.; Sherwin, B.D.; Ferreira E.G.M. Restoring cosmological concordance with early dark energy and massive neutrinos? *arXiv* **2022**, arXiv:2207.01501.
6. Verde, L.; Treu, T.; Riess, A.G. Tensions between the Early and the Late Universe. *Nat. Astron.* **2019**, *3*, 891. [[CrossRef](#)]
7. Vagnozzi, S. Consistency tests of Λ CDM from the early integrated Sachs-Wolfe effect: Implications for early-time new physics and the Hubble tension. *Phys. Rev. D* **2021**, *104*, 063524. [[CrossRef](#)]
8. Perivolaropoulos, L.; Skara, F. Hubble tension or a transition of the Cepheid SnIa calibrator parameters? *Phys. Rev. D* **2021**, *104*, 123511 [[CrossRef](#)]
9. Vagnozzi, S.; Pacucci, F.; Loeb, A. Implications for the Hubble tension from the ages of the oldest astrophysical objects. *JHEAp* **2022**, *36*, 27–35 [[CrossRef](#)]
10. Perivolaropoulos, L. Is the Hubble crisis connected with the extinction of dinosaurs? *arXiv* **2022**, arXiv:2201.08997.
11. Odintsov, S.D.; Oikonomou, V.K. Did the Universe Experienced a Pressure non-Crushing Type Cosmological Singularity in the Recent Past? *arXiv* **2022**, arXiv:2201.07647.
12. Odintsov, S.D.; Oikonomou, V.K. Dissimilar Donuts in the Sky? Effects of a Pressure Singularity on the Circular Photon Orbits and Shadow of a Cosmological Black Hole. *arXiv* **2022**, arXiv:2208.07972.
13. Niedermann, F.; Sloth, M.S. Resolving the Hubble tension with new early dark energy. *Phys. Rev. D* **2020**, *102*, 063527. [[CrossRef](#)]
14. Poulin, V.; Smith, T.L.; Karwal, T.; Kamionkowski, M. Early Dark Energy Can Resolve The Hubble Tension. *Phys. Rev. Lett.* **2019**, *122*, 221301. [[CrossRef](#)]
15. Karwal, T.; Kamionkowski, M. Dark energy at early times, the Hubble parameter, and the string axiverse. *Phys. Rev. D* **2016**, *94*, 103523. [[CrossRef](#)]
16. Oikonomou, V.K. Unifying inflation with early and late dark energy epochs in axion $F(R)$ gravity. *Phys. Rev. D* **2021**, *103*, 044036. [[CrossRef](#)]
17. Nojiri S., Odintsov S.D.; Oikonomou V.K., Unifying Inflation with Early and Late-time Dark Energy in $F(R)$ Gravity. *Phys. Dark Univ.* **2020**, *29*, 100602. [[CrossRef](#)]
18. Mortsell, E.; Goobar, A.; Johansson, J.; Dhawan, S. The Hubble Tension Bites the Dust: Sensitivity of the Hubble Constant Determination to Cepheid Color Calibration. *arXiv* **2021**, arXiv:2105.11461.
19. Dai, W.M.; Ma, Y.Z.; He, H.J. Reconciling Hubble Constant Discrepancy from Holographic Dark Energy. *Phys. Rev. D* **2020**, *102*, 121302. [[CrossRef](#)]
20. He, H.J.; Ma, Y.Z.; Zheng, J. Resolving Hubble Tension by Self-Interacting Neutrinos with Dirac Seesaw. *JCAP* **2020**, *11*, 3. [[CrossRef](#)]
21. Nakai, Y.; Suzuki, M.; Takahashi, F.; Yamada, M. Gravitational Waves and Dark Radiation from Dark Phase Transition: Connecting NANOGrav Pulsar Timing Data and Hubble Tension. *Phys. Lett. B* **2021**, *816*, 136238. [[CrossRef](#)]

22. Di Valentino E., Mukherjee A.; Sen A.A., Dark Energy with Phantom Crossing and the H_0 Tension. *Entropy* **2021**, *23*, 404. [\[CrossRef\]](#) [\[PubMed\]](#)
23. Agrawal, P.; Obied, G.; Vafa, C. H_0 tension, swampland conjectures, and the epoch of fading dark matter. *Phys. Rev. D* **2021**, *103*, 043523. [\[CrossRef\]](#)
24. Yang, W.; Pan, S.; Di Valentino, E.; Nunes, R.C.; Vagnozzi, S.; Mota, D.F. Tale of stable interacting dark energy, observational signatures, and the H_0 tension. *JCAP* **2018**, *9*, 19. [\[CrossRef\]](#)
25. Ye, G.; Piao, Y.S. Is the Hubble tension a hint of AdS phase around recombination? *Phys. Rev. D* **2020**, *101*, 083507. [\[CrossRef\]](#)
26. Desmond, H.; Jain, B.; Sakstein, J. Local resolution of the Hubble tension: The impact of screened fifth forces on the cosmic distance ladder. *Phys. Rev. D* **2019**, *100*, 043537; Erratum in *Phys. Rev. D* **2020**, *101*, 069904; Erratum in *Phys. Rev. D* **2020**, *101*, 129901. [\[CrossRef\]](#)
27. Di Valentino, E.; Melchiorri, A.; Mena, O.; Vagnozzi, S. Nonminimal dark sector physics and cosmological tensions. *Phys. Rev. D* **2020**, *101*, 063502. [\[CrossRef\]](#)
28. Colgáin, E.Ó.; van Putten, M.H.P.M.; Yavartanoo, H.; de Sitter, Swampland, H_0 tension & observation. *Phys. Lett. B* **2019**, *793*, 126–129
29. Vagnozzi, S. New physics in light of the H_0 tension: An alternative view. *Phys. Rev. D* **2020**, *102*, 023518. [\[CrossRef\]](#)
30. Krishnan, C.; Colgáin, E.Ó.; Sen, A.A.; Sheikh-Jabbari, M.M.; Yang, T. Is there an early Universe solution to Hubble tension? *Phys. Rev. D* **2020**, *102*, 103525. [\[CrossRef\]](#)
31. Di Valentino, E.; Melchiorri, A.; Mena, O.; Vagnozzi, S. Interacting dark energy in the early 2020s: A promising solution to the H_0 and cosmic shear tensions. *Phys. Dark Univ.* **2020**, *30*, 100666. [\[CrossRef\]](#)
32. Colgáin, E.Ó.; Yavartanoo, H. Testing the Swampland: H_0 tension. *Phys. Lett. B* **2019**, *797*, 134907. [\[CrossRef\]](#)
33. Lee, B.H.; Lee, W.; ÓColgáin, E.; Sheikh-Jabbari, M.M.; Thakur, S. Is Local H_0 At Odds With Dark Energy EFT? *arXiv* **2022**, arXiv:2202.03906.
34. Nojiri, S.; Odintsov, S.D.; Gomez, D.S.C.; Sharov, G.S. Modeling and testing the equation of state for (Early) dark energy. *Phys. Dark Univ.* **2021**, *32*, 100837. [\[CrossRef\]](#)
35. Krishnan, C.; Mohayaee, R.; Colgáin, E.Ó.; Sheikh-Jabbari, M.M.; Yin, L. Does Hubble tension signal a breakdown in FLRW cosmology? *Class. Quant. Grav.* **2021**, *38*, 184001. [\[CrossRef\]](#)
36. Ye, G.; Zhang, J.; Piao, Y.S. Resolving both H_0 and S_8 tensions with AdS early dark energy and ultralight axion. *arXiv* **2021**, arXiv:2107.13391.
37. Ye, G.; Piao, Y.S. Improved constraint on primordial gravitational waves in light of the Hubble tension and BICEP/Keck. *arXiv* **2022**, arXiv:2202.10055.
38. Marra, V.; Perivolaropoulos, L. Rapid transition of G_{eff} at $z \simeq 0.01$ as a possible solution of the Hubble and growth tensions. *Phys. Rev. D* **2021**, *104*, L021303. [\[CrossRef\]](#)
39. McVittie, G.C. The mass-particle in an expanding universe. *Mon. Not. Roy. Astron. Soc.* **1933**, *93*, 325–339. [\[CrossRef\]](#)
40. Faraoni, V.; Jacques, A. Cosmological expansion and local physics. *Phys. Rev. D* **2007**, *76*, 063510. [\[CrossRef\]](#)
41. Kaloper, N.; Kleban, M.; Martin, D. McVittie’s Legacy: Black Holes in an Expanding Universe. *Phys. Rev. D* **2010**, *81*, 104044. [\[CrossRef\]](#)
42. Lake, K.; Abdelqader, M. More on McVittie’s Legacy: A Schwarzschild—de Sitter black and white hole embedded in an asymptotically Λ CDM cosmology. *Phys. Rev. D* **2011**, *84*, 044045. [\[CrossRef\]](#)
43. Nandra, R.; Lasenby, A.N.; Hobson, M.P. The effect of an expanding universe on massive objects. *Mon. Not. Roy. Astron. Soc.* **2012**, *422*, 2945–2959. [\[CrossRef\]](#)
44. Nolan, B.C. Particle and photon orbits in McVittie spacetimes. *Class. Quant. Grav.* **2014**, *31*, 235008. [\[CrossRef\]](#)
45. Maciel, A.; Guariento, D.C.; Molina, C. Cosmological black holes and white holes with time-dependent mass. *Phys. Rev. D* **2015**, *91*, 084043. [\[CrossRef\]](#)
46. Nolan, B.C. Local properties and global structure of McVittie spacetimes with non-flat Friedmann–Lemaître–Robertson–Walker backgrounds. *Class. Quant. Grav.* **2017**, *34*, 225002. [\[CrossRef\]](#)
47. Perlick, V.; Tsupko, O.Y.; Isnovaty-Kogan, G.S.B. Black hole shadow in an expanding universe with a cosmological constant. *Phys. Rev. D* **2018**, *97*, 104062. [\[CrossRef\]](#)
48. Pérez, D.; Perez Bergliaffa, S.E.; Romero, G.E. Dynamical black hole in a bouncing universe. *Phys. Rev. D* **2021**, *103*, 064019. [\[CrossRef\]](#)
49. Bisnovaty-Kogan, G.S.; Tsupko, O.Y. Shadow of a black hole at cosmological distances. *Phys. Rev. D* **2018**, *98*, 084020. [\[CrossRef\]](#)
50. Tsupko, O.Y.; Bisnovaty-Kogan, G.S. First analytical calculation of black hole shadow in McVittie metric. *Int. J. Mod. Phys. D* **2020**, *29*, 2050062. [\[CrossRef\]](#)
51. Pérez, D.; Romero, G.E.; Combi, L.E.; Gutiérrez, E. A note on geodesics in inhomogeneous expanding spacetimes. *Class. Quant. Grav.* **2019**, *36*, 055002. [\[CrossRef\]](#)
52. Perlick, V.; Tsupko, O.Y. Calculating black hole shadows: Review of analytical studies. *Phys. Rept.* **2022**, *947*, 1–39. [\[CrossRef\]](#)
53. Nojiri, S.; Odintsov, S.D.; Faraoni, V. Searching for dynamical black holes in various theories of gravity. *Phys. Rev. D* **2021**, *103*, 044055. [\[CrossRef\]](#)
54. Vagnozzi, S.; Visinelli, L. Note on Fundamental Physics Tests from Black Hole Imaging: Comment on “Hunting for Extra Dimensions in the Shadow of Sagittarius A^{**}”. *Res. Notes AAS* **2022**, *6*, 106. [\[CrossRef\]](#)

55. Vagnozzi, S.; Roy, R.; Tsai, Y.D.; Visinelli, L.; Afrin, M.; Allahyari, A.; Bambhaniya, P.; Dey, D.; Ghosh, S.G.; Joshi, P.S.; et al. Horizon-scale tests of gravity theories and fundamental physics from the Event Horizon Telescope image of Sagittarius A*. *arXiv* **2022**, arXiv:2205.07787.
56. Chen, Y.; Roy, R.; Vagnozzi, S.; Visinelli, L. Superradiant evolution of the shadow and photon ring of Sgr A*. *arXiv* **2022**, arXiv:2205.06238.
57. Roy, R.; Vagnozzi, S.; Visinelli, L. Superradiance evolution of black hole shadows revisited. *Phys. Rev. D* **2022**, *105*, 083002. [[CrossRef](#)]
58. Khodadi, M.; Allahyari, A.; Vagnozzi, S.; Mota, D.F. Black holes with scalar hair in light of the Event Horizon Telescope. *JCAP* **2020**, *9*, 26. [[CrossRef](#)]
59. Vagnozzi, S.; Bambi, C.; Visinelli, L. Concerns regarding the use of black hole shadows as standard rulers. *Class. Quant. Grav.* **2020**, *37*, 087001. [[CrossRef](#)]
60. Allahyari, A.; Khodadi, M.; Vagnozzi, S.; Mota, D.F. Magnetically charged black holes from non-linear electrodynamics and the Event Horizon Telescope. *JCAP* **2020**, *2*, 3. [[CrossRef](#)]
61. Bambi, C.; Freese, K.; Vagnozzi, S.; Visinelli, L. Testing the rotational nature of the supermassive object M87* from the circularity and size of its first image. *Phys. Rev. D* **2019**, *100*, 044057. [[CrossRef](#)]
62. Nojiri, S.; Odintsov, S.D.; Tsujikawa, S. Properties of singularities in (phantom) dark energy universe. *Phys. Rev. D* **2005**, *71*, 063004. [[CrossRef](#)]
63. Caldwell, R.R.; Kamionkowski, M.; Weinberg, N.N. Phantom Energy and Cosmic Doomsday. *Phys. Rev. Lett.* **2003**, *91*, 071301. [[CrossRef](#)] [[PubMed](#)]
64. Nojiri, S.; Odintsov, S.D. Quantum deSitter cosmology and phantom matter. *Phys. Lett. B* **2003**, *562*, 147. [[CrossRef](#)]
65. Faraoni, V. Superquintessence. *Int. J. Mod. Phys. D* **2002**, *11*, 471. [[CrossRef](#)]
66. Barrow, J.D. Sudden future singularities. *Class. Quant. Grav.* **2004**, *21*, L79. [[CrossRef](#)]
67. Nojiri, S.; Odintsov, S.D. Quantum escape of sudden future singularity. *Phys. Lett. B* **2004**, *595*, 1. [[CrossRef](#)]
68. Barrow, J.D.; Tsagas, C.G. New Isotropic and Anisotropic Sudden Singularities. *Class. Quant. Grav.* **2005**, *22*, 1563. [[CrossRef](#)]
69. Fernandez-Jambrina, L.; Lazkoz, R. Geodesic behavior of sudden future singularities. *Phys. Rev. D* **2004**, *70*, 121503. [[CrossRef](#)]
70. Bouhmadi-Lopez, M.; Gonzalez-Diaz, P.F.; Martin-Moruno, P. Worse than a Big Rip? *Phys. Lett. B* **2008**, *659*, 1. [[CrossRef](#)]
71. Nojiri, S.; Odintsov, S.D. The Final state and thermodynamics of dark energy universe. *Phys. Rev. D* **2004**, *70*, 103522. [[CrossRef](#)]
72. Nojiri, S.; Odintsov, S.D.; Oikonomou, V.K. Quantitative analysis of singular inflation with scalar-tensor and modified gravity. *Phys. Rev. D* **2015**, *91*, 084059. [[CrossRef](#)]
73. Odintsov, S.D.; Oikonomou, V.K. Bouncing cosmology with future singularity from modified gravity. *Phys. Rev. D* **2015**, *92*, 024016. [[CrossRef](#)]
74. Oikonomou, V.K. Singular Bouncing Cosmology from Gauss-Bonnet Modified Gravity. *Phys. Rev. D* **2015**, *92*, 124027. [[CrossRef](#)]
75. Oikonomou, V.K. Constraints on Singular Evolution from Gravitational Baryogenesis. *Int. J. Geom. Meth. Mod. Phys.* **2016**, *13*, 1650033. [[CrossRef](#)]
76. Perivolaropoulos, L. Fate of bound systems through sudden future singularities. *Phys. Rev. D* **2016**, *94*, 124018. [[CrossRef](#)]
77. Bamba, K.; Lopez-Revelles, A.; Myrzakulov, R.; Odintsov, S.D.; Sebastiani, L. Cosmic history of viable exponential gravity: Equation of state oscillations and growth index from inflation to dark energy era. *Class. Quant. Grav.* **2013**, *30*, 015008. [[CrossRef](#)]
78. Nesseris, S.; Perivolaropoulos, L. The Fate of bound systems in phantom and quintessence cosmologies. *Phys. Rev. D* **2004**, *70*, 123529. [[CrossRef](#)]
79. Akiyama, K. [Event Horizon Telescope]. First M87 Event Horizon Telescope Results. I. The Shadow of the Supermassive Black Hole. *Astrophys. J. Lett.* **2019**, *875*, L1.
80. Akiyama, K. [Event Horizon Telescope]. First M87 Event Horizon Telescope Results. VI. The Shadow and Mass of the Central Black Hole. *Astrophys. J. Lett.* **2019**, *875*, L6.
81. Akiyama, K. [Event Horizon Telescope]. First Sagittarius A* Event Horizon Telescope Results. I. The Shadow of the Supermassive Black Hole in the Center of the Milky Way. *Astrophys. J. Lett.* **2022**, *930*, L12.
82. Capozziello, S.; Dialektopoulos, K.F.; Luongo, O. Maximum turnaround radius in $f(R)$ gravity. *Int. J. Mod. Phys. D* **2018**, *28*, 1950058. [[CrossRef](#)]
83. Capozziello, S.; Farooq, O.; Luongo, O.; Ratra, B. Cosmographic bounds on the cosmological deceleration-acceleration transition redshift in $f(R)$ gravity. *Phys. Rev. D* **2014**, *90*, 044016. [[CrossRef](#)]
84. Mortlock, D.J.; Warren, S.J.; Venemans, B.P.; Patel, M.; Hewett, P.C.; McMahon, R.G.; Simpson, C.; Theuns, T.; Gonzales-Solares, E.A.; Adamson, A.; et al. A luminous quasar at a redshift of $z = 7.085$. *Nature* **2011**, *474*, 616. [[CrossRef](#)] [[PubMed](#)]
85. Younsi, Z.; Zhidenko, A.; Rezzolla, L.; Konoplya, R.; Mizuno, Y. New method for shadow calculations: Application to parametrized axisymmetric black holes. *Phys. Rev. D* **2016**, *94*, 084025. [[CrossRef](#)]
86. Abdujabbarov, A.A.; Rezzolla, L.; Ahmedov, B.J. A coordinate-independent characterization of a black hole shadow. *Mon. Not. Roy. Astron. Soc.* **2015**, *454*, 2423–2435. [[CrossRef](#)]
87. Addazi, A.; Capozziello, S.; Odintsov, S. Chaotic solutions and black hole shadow in $f(R)$ gravity. *Phys. Lett. B* **2021**, *816*, 136257. [[CrossRef](#)]
88. Miranda, M.; Vernieri, D.; Capozziello, S.; Faraoni, V. Generalized McVittie geometry in Horndeski gravity with matter. *Phys. Rev. D* **2022**, *105*, 124024. [[CrossRef](#)]